Printability and fire performance of a developed 3D printable fiber reinforced cementitious composite under elevated temperatures

Yiwei Weng[a,b], Mingyang Li[a], Zhixin Liu[a], Wenxin Lao[a], Bing Lu[a,b], Dong Zhang[b], Ming Jen Tan[a]

[a]Singapore Centre for 3D Printing, School of Mechanical and Aerospace Engineering, Nanyang Technological University, Singapore

[b]School of Civil and Environmental Engineering, Nanyang Technological University, Singapore

ABSTRACT:

To demonstrate printability and fire performance of 3D printable fiber reinforced cementitious materials at elevated temperatures, large-scaling printing and fire performance testing are required for engineering applications. In this work, a mixture design of 3D printable fiber reinforced cementitious composite (3DPFRCC) for large-scale printing was developed. A structure with dimensions of 78 × 60 × 90 cm (L × W × H) was printed by a gantry printer in 150 minutes, which demonstrates that the developed 3DPFRCC mixture possesses good buildability. The rheological property, setting-time, and mechanical properties under normal and elevated temperatures of the developed 3DPFRCC were then characterized. Final results indicate that the developed 3DPFRCC is suitable for engineering applications due to its good printability and mechanical properties under normal and elevated temperatures.

Keywords: 3D printing; fiber reinforced cementitious materials; rheological properties; large-scale printing; high temperatures

1. Introduction

3D printing for building sand construction builds up structures in a layer-atop-layer manner according to designed CAD models (Bos, Rob, et al. 2016; Chua, Leong, and Lim 2003; Davtalab, Kazemian, and Khoshnevis 2018; Jiang et al. 2018; Li et al. 2016; Lim et al. 2018b; Weng et al. 2016; Xia and Sanjayan 2016, 2018). In the 3D printing process, cementitious materials should be pumpable and buildable, which can be determined by the rheological properties of materials at fresh state (Li et al. 2013; Weng, et al. 2016; Lim, Panda, and Pham 2018; Lu et al. 2018; Panda and Tan 2018; Salet et al. 2018; Tay et al. 2017, 2018; Weng et al. 2018 a; X. Zhang et al. 2018). Pumpable means how easily the materials can be conveyed in the delivering system, which requires low yield stress and low plastic viscosity of material (Chhabra and Richardson 1959). Buildable means how stably the materials can be stacked together, which requires high yield stress and high Young's modulus of the material (Perrot, Rangeard, and Pierre 2016; Wolfs, Bos, and Salet 2018). Therefore, the main challenge of developing a 3D printable cementitious material would be finding the narrow window to satisfy the requirements of both pumpability and buildability (Weng et al. 2018 b).

While some research has reported the development of 3D printable plain concrete (Bos, Wolfs, et al. 2016; Le et al. 2012; S. Lim et al. 2012). plain concrete is still a type of brittle materials with low tensile strength and crack resistance. Cracks, as shown in Figure 1, is always a concern to adopting such material into engineering applications. As short fibers are ideal ingredients to enhance the mechanical property of cementitious materials and restrain cracks caused by dry shrinkage in casting concrete (Tang et al. 2015), a number of researchers have worked on developing appropriate types of 3DPFRCCs with different types of fibers or dosages (Hambach and Volkmer 2017; Soltan and Li 2018). However, several limitations remained in formerly developed materials obstruct further implementation of these materials in engineering

applications. Firstly, large-scale printing is missing in previous studies to test the printability of developed materials with actual engineering work setup. A number of challenges exist when upscale from lab scale printing to real building scale printing, e.g. the requirements of pumpability and buildability become more restrict as the scales of equipment and printing become much larger, the setting time of materials should be tailored such that the materials possess proper hydration rate for 3D printing, the mixing procedure should be able to meet the material consumption rate of printing, etc. (Weng et al. 2018a). Secondly, the characterization of mechanical properties of 3DPFRCCs is lacking, which is problematic considering that proper material characterization serves as a guideline to inform engineering applications. Thirdly, much more attention should be paid to the fire performance of newly developed 3DPFRCCs for better adoption rates for use in relevant applications, especially when material properties and structural safety are known to deteriorate and behave erratically at high temperatures (Dong, Kang Hai, and Aravind 2018; Liu and Tan 2018; D. Zhang, Dasari, and Tan 2018). To overcome these issues, a comprehensive work should be carried out to investigate all the aforementioned aspects for developed 3DPFRCCs.

Figure 1 Cracks form on the surface of the printed structure

In the study, a novel mixture of 3DPFRCCs is developed, and a 90 cm high structure was printed to demonstrate the printability of developed materials. To the authors' knowledge, currently this is the highest 3D printed structure with notable short fiber reinforced materials around the world in the academia. Rheological properties were characterized by static/dynamic yield stress and plastic viscosity. Workable time of materials for 3D printing was characterized by setting time (Weng et al. 2018a). The mechanical properties (flexural and compressive strength) were tested at both normal and elevated temperatures. Besides, spalling effect and Young's modulus were also explored.

2. Experimental design

2.1 Materials and mixing

In this study, the mixture consists of Ordinary Portland Cement type I 42.5 (C), natural river sand (S), class F fly ash with a fineness of 386 m_2/kg (FA), silica fume (SF, undensified, Grade 940, Elkem company), and polyvinyl alcohol (PVA) fiber with 40 μm in diameter, 8 mm in length and 0.8% oil coating. Superplasticizer was introduced with the dosage of 3 g/L to adjust the rheological properties. These raw ingredients are wide sourcing in civil engineering. Specifically, fly ash and silica fume are the industrial by-products, which were reused for 3D concrete printing resulting in decreased cost and increased sustainability of the process (Ruan and Unluer 2017). Physical and chemical properties of OPC, fly ash, and silica fume are shown in Figure 2 and Table 1. The gradation curve of natural river sand is shown in Figure 3. The influence of each ingredient on rheological properties was studied in the author's previous work (Weng, et al. 2018 a). The mixture proportion is listed in Table 2 (Weng, et al. 2018).

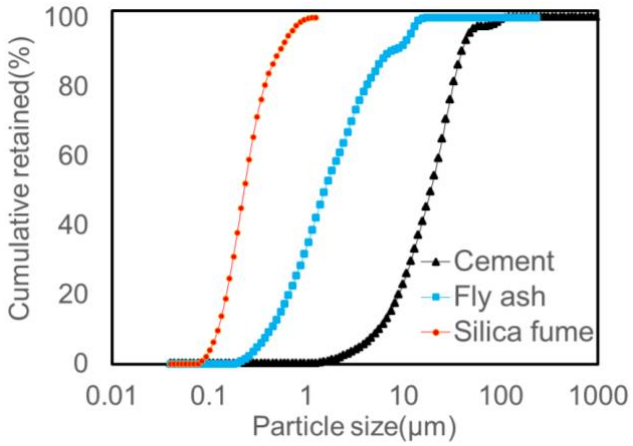

92

93 Figure 2 Particle size distribution of cement, fly ash and silica fume

94

95 Table 1 Chemical composition of fly ash and Ordinary Portland Cement (C)

Formula	Concentration / %	
	Fly ash	Cement
SiO_2	58.59	24.27
Al_2O_3	30.44	4.56
Fe_2O_3	4.66	3.95
TiO_2	2.02	0.55
K_2O	1.51	0.61
CaO	1.21	62.2
MgO	0.776	3.34
P_2O_5	0.531	0.15
Na_2O	-	0.21
SO_3	0.0914	-
ZrO_2	0.04	-
MnO	0.0351	-
Cr_2O_3	0.027	-

CuO	0.0254	-
ZnO	0.0229	-

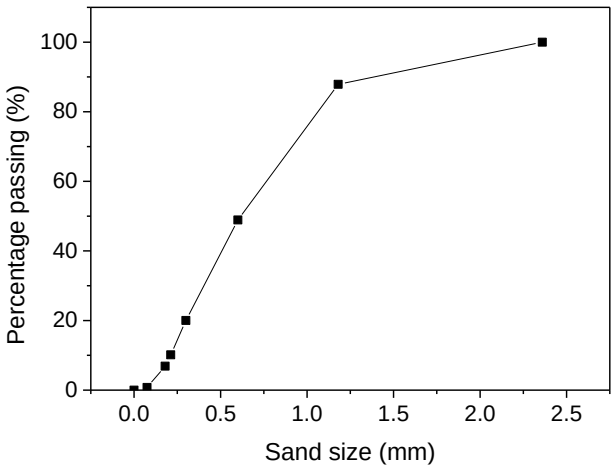

Figure 3 Gradation curve of sand particles

Table 2 Mixture proportions

S/B[a]	W/B	FA/C	SF/%	Fiber/%
0.5	0.28	1.0	0.05	1

[a] B indicates the binder that is the sum weight of C, FA, and SF

An 80L Screed Mortar Mixer (Soroto) was used to mix raw ingredients. As rheological properties are affected by many external factors, such as temperature, mixing time, etc (Ruan et al. 2018; Yang et al. 2009), the mixing process is fixed to ensure the consistency of rheological properties of materials (Weng et al. 2018 a). Firstly, the powder of all solid ingredients was dry mixed for 1 min with stir speed. Water was then added with the mixing process continued for 1 minute with stir speed. After that, the superplasticizer was introduced, the mixing process continued for 1 minute in speed I followed by 1 minute with speed II. Finally, the fiber is introduced, and the mixing process continued for 2 minutes with speed II.

2.2 Rheological characterization

Bingham model is a classic rheological model of cementitious materials. According to the Bingham model, fresh cementitious materials can flow after it overcomes its static yield stress. During the flow, dynamic yield stress is the minimum yield stress to maintain its flow. The plasticity viscosity measures how easily the materials can flow once the yield stress is overcome.

In this study, the rheological performance was characterized by a Viskomat XL with a six-blade vane probe and a cage, the detailed dimension of the probe, cage, and testing program were introduced in authors' previous work (Weng et al., 2018 b). An example of rheology test results is plotted in Figure 4.

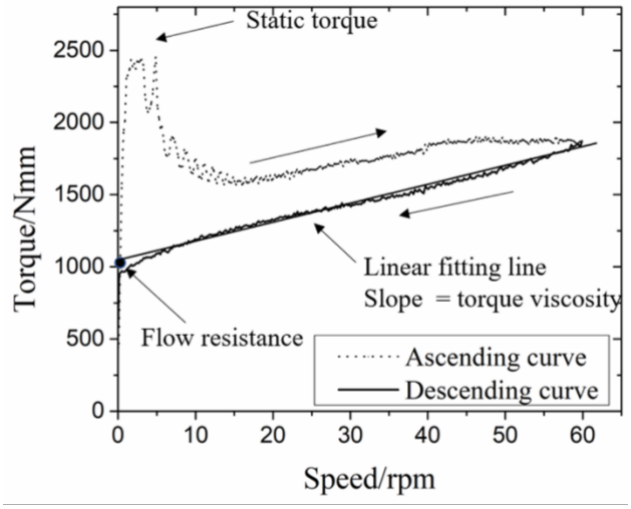

Figure 4 An example of rheology test results

Then, the static/dynamic torque and torque viscosity can be converted into static/dynamic yield stress and plastic viscosity via the following equation:

$$\Gamma = \frac{4\pi R_1^2 R_2{}^2 l\eta}{R_2{}^2 - R_1{}^2}\omega_2 - \frac{4\pi R_1^2 R_2{}^2 l\tau_0}{R_2{}^2 - R_1{}^2}\ln\frac{R_1}{R_2} \quad (1)$$

where Γ (N·m) is the torque, ω_2 (rad/s) is the rotational speed of outer barrel, l (m) and R_1 (m) are the length and radius of the probe, respectively, and R_2 (m) is the radius of the outer barrel.

Setting time is another essential parameter, which determines the workable time of 3DPFRCC in the printing process. In this work, the setting time of the cement pastes was determined according to ASTM C 191-13 with an automatic Vicat apparatus. A specimen of normal consistency fresh cement paste was prepared and placed in a 40 mm high container with a diameter of 40 mm. A 1.13 diameter needle fixed on a movable rod penetrated the specimen every 4 minutes, and the penetration depth of the needle was measured. The initial setting time in this study was calculated from follows:

$$\text{Initial setting time} = \frac{(H-E)}{(C-D)} \times (C-25) + E \quad (2)$$

where E (min) is the time of last penetration greater than 25 mm; H (min) is the time of first penetration less than 25 mm; C (mm) and D (mm) are the penetration depth reading at time E and H, respectively.

2.3 Printing test

The printing test was conducted by a gantry printer with a printing volume of 1.2 m × 1.2 m × 1.0 m (L × W × H). The printer, which has the largest print capacity in the authors' lab, is shown in Figure 5. To demonstrate the advantage of customization in 3D printing, a special structure was designed and shown in Figure 6, which illustrates the top-view and overall-view of the 3D model for printing. The detailed dimension is shown in Figure 6 (a). The height of the printed structure is 90 cm due to the capacity limitation of the printer.

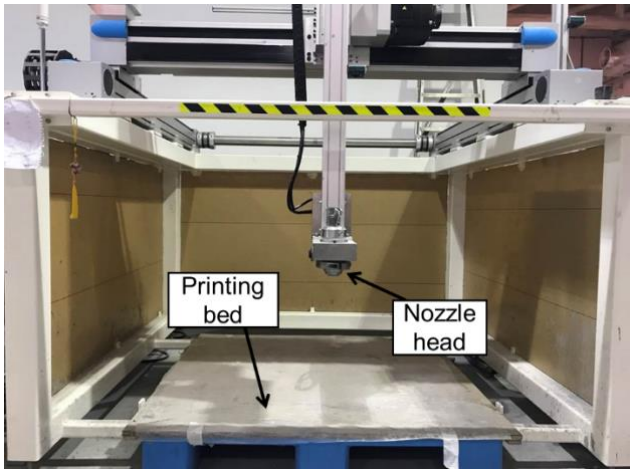

Figure 5 Gantry printer

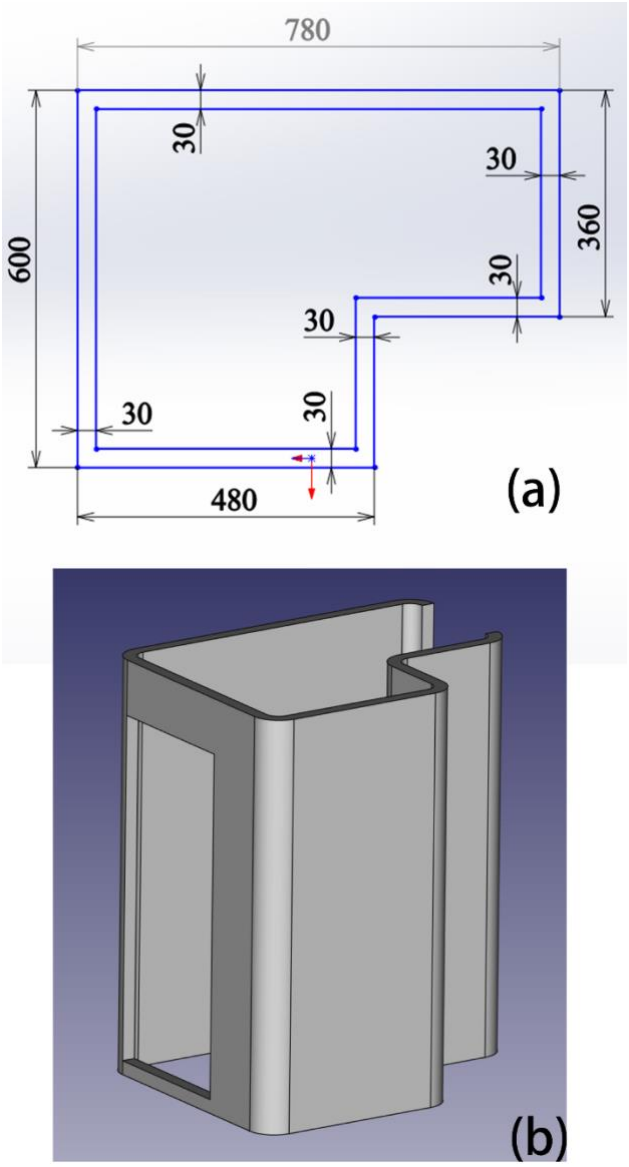

Figure 6 3D printing model: (a) top-view of the designed part; (b) overall-view of the designed part

2.4 Characterization of mechanical properties and fire properties

Three cylinders with a diameter of 50 mm and a height of 100 mm were adopted for each spalling test, which was conducted in an electrical furnace. During the test, the furnace was heated according to the standard heating curve of ISO 834 for 1 h as shown in Figure 7 (Liu and Tan 2018), and then naturally cooled down to room temperature for 24 h. The extent of spalling on the cylinders was visually observed. To estimate the influence of fibers on

mechanical performance of 3DPFRCCs, a control group was also prepared besides specimens fabricated with 3DPFRCCs. The control group possesses the same formulation as shown in Table 2 except that the fiber dosage is null. Young's modulus test was conducted with cylinder specimens having the same dimensions, materials and heating curve.

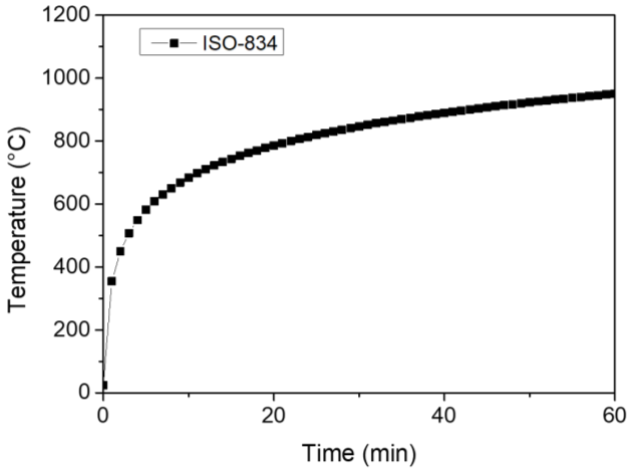

Figure 7 Heating curve for spalling test

Flexural and compressive specimens were printed with the gantry concrete printer. The nozzle used for printing was 30 mm × 15 mm (L × W). The printing and pumping speed were 4000 mm/min and 1.8 L/min, respectively. The standoff distance was 15 mm for each layer. In order to avoid the effect of material property time dependency and batch-to-batch inconsistency, all the testing samples were printed together continuously. For the flexural test, the printed 2 layers (totally 30 mm in height) filaments were cut into separate specimens with 350 mm in length due to the limitation of equipment capacity for testing (Weng et al., 2018 b). Afterwards, a four-point bending test with a span length of 240 mm was conducted at 28 days. For the compressive test, the printed 2×4 layers (totally 60 mm in both width and height) filaments were cut into 50 mm × 50 mm × 50 mm (L × W × H) cubic specimens (Weng et al. 2018 b). Then these cubic specimens were subjected to the following isothermal temperatures: 25 °C

(ambient temperature), 200 °C, 400 °C, 600 °C and 800 °C. The compressive strength was measured by uniaxial loading in triplicates at 28 days in accordance with the specifications of ASTM C109/C109M-13. The equipment used for this purpose was a Toni Technik Baustoffprüfsysteme machine with a loading rate of 100 KN/min.

3. Results and discussions

3.1 Large scale printing

The results of the rheological test are presented in Table 3. The result of setting time is shown in Figure 8. According to Figure 8 and Eqn. (2), the initial setting time is 59.2 mins. The static and dynamic yield stress are 3289 Pa and 314.7 Pa, respectively, and the plastic viscosity is 32.5 Pa·s. According to Weng et al.'s work, materials are able to support the weight of printed structure with 300 mm height at fresh state when its static yield stress is above 3000 Pa.

Table 3 Testing results of rheological and mechanical performance

Rheological parameters	Results
Plastic Viscosity / Pa·s	32.5
Static Yield Stress / Pa	3289
Dynamic Yield Stress / Pa	314.7

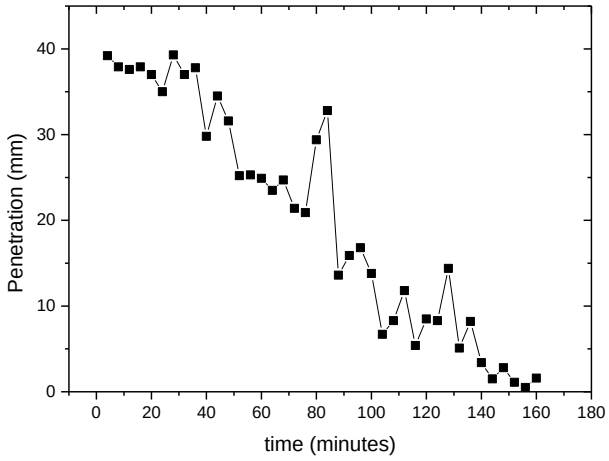

Figure 8 Setting time test result

The large-scale printing test result is shown in Figure 9. In the printing process, the standoff distance was 10 mm for each layer. A concrete plate with 400 mm × 35 mm × 15 mm (L × W × H) was preprinted to support the overhang structure.

In the large-scale printing process, when materials are at a fresh state, the printed height is limited within 300 mm, which is a safety height according to rheological properties in terms of static yield stress. After materials reach initial setting, the development rate of material property to sustain the weight of subsequent layers evolves extremely fast compared with that of materials at fresh state (Lowke 2018; Roussel 2006; Wang et al. 2018) such that the printer can build up higher structure than 300 mm without collapse.

Therefore, the printed height of 300 mm takes around 50 mins in the printing process. When the printed height is more than 300 mm, materials have reached an initial setting state where material properties develop fast, which is desirable for the large-scale printing. The whole printing process lasted 150 min. The printing result indicates that developed 3DPFRCCs possesses appropriate rheological properties for a meter-level printing and has the potential for the future engineering application.

Figure 9 Large-scale printing with the dimension of 78 cm × 60 cm × 90 cm (L × W × H)

3.2 Characterization of fire performance

Results of the spalling test are shown in Figure 10. As can be seen from Figure 10 (a), 3DPFRCCs can maintain its structure after the spalling test, and only small cracks can be found on the specimen surface. However, as shown in Figure 10 (b), plain concrete is potentially explosive, which is undesirable for the building application. The phenomenon indicates that the addition of PVA fibers is an effective approach to preventing spalling of 3DPFRCCs, since the microcrack forms in specimens when PVA fibers expand, melt and evaporate at high

230 temperature such that microchannels form inside specimens, which is beneficial for water
231 evaporation to avoid spalling effect (Zhang et al., 2018).
232

233

234 Figure 10 Results of spalling test: (a) 3DPFRCC; (b) 3DP plain concrete
235

236 The result of Young's modulus is plotted in Figure 11. The Young's modulus of both
237 3DPFRCCs and plain concrete decreases dramatically after the spalling test. However,
238 Young's modulus of 3DPFRCCs is 25 % higher than that of plain concrete at ambient
239 temperature. The results of Young's modulus test after the high temperature in this work is
240 comparable with Carino and Pham's work (T.Pham and J.Carino 2012).

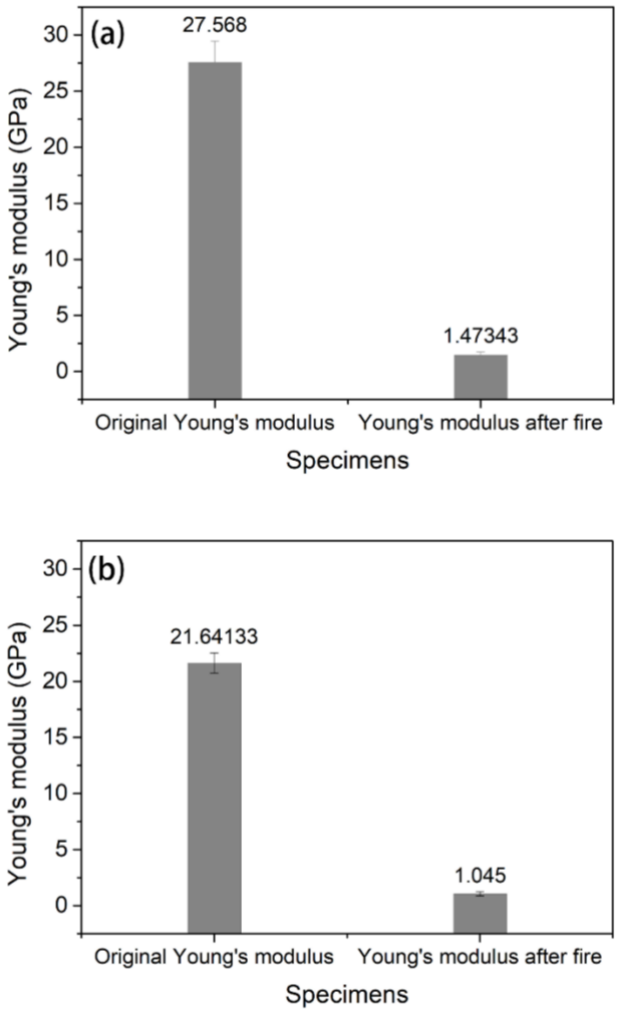

Figure 11 Residual young's modulus: (a) 3DPFRCC; (b)3DP plain concrete

Figure 12 plots the mechanical property of 3DPFRCCs and plain concrete as a function of isothermal temperatures. Figure 12 (a) depicts the result of compressive strength at elevated temperatures. Dehydration of cement paste by driving out of physically bound water at around 110 °C such that microcracks form inside specimens and mechanical performance deteriorates. Then, the evaporation gas releases at around 300 °C. Water vaporizes at a temperature less than 300 °C, consequently resulting in an increase in concrete porosity and the creation of more escape routes. Therefore, water vapor pressure in materials reduces. Furthermore, the

evaporation of water vapor is beneficial for hydration process and can improve the compressive strength of materials (Zheng, Luo, and Wang 2014). However, the mechanical performance decreases drastically at 800 ℃ where the mechanical performance becomes less than half. It is because that C-S-H is unstable at high temperature (Arioz 2007). Consequently, the mechanical property deteriorates at high temperature as C-S-H is the main contributor of mechanical property in cementitious materials. The residual compressive strength was 30 MPa and 31 MPa for plain concrete and 3DPFRCCs, respectively.

The flexural strength of materials as a function of temperature is shown in Figure 12 (b). The flexural strength decreases almost linearly with increasing temperature from 200 °C to 800 °C. Losses in flexural strength result from cracks and pores due to the evaporation of free water and bound water (Khoury 1992). The residual flexural strength was 1.5 MPa and 2.1 MPa for plain concrete and 3DPFRCCs, respectively.

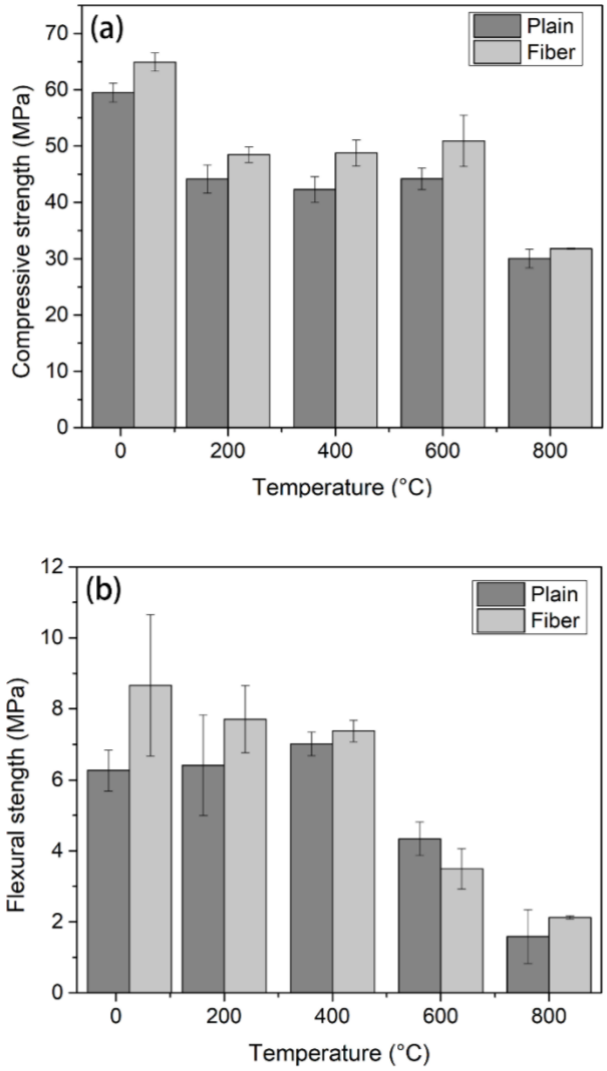

Figure 12 Mechanical properties at elevated temperature

4. Conclusions

3D printable cementitious composites require special rheological properties to satisfy the demand of printability (buildability and pumpability). In this work, a novel mixture of 3D printable fiber reinforced cementitious composites (3DPFRCCs) is developed and is capable of large-scale printing, which is verified by printing test. A 78 × 60 × 90 cm (L × W × H) structure was printed successfully within 150 minutes, which demonstrates that this novel 3DPFRCCs possess excellent buildability and pumpability.

Rheological properties, setting-time, mechanical properties, and fire properties were characterized. Results indicate that the developed material possesses appropriate rheological and mechanical properties for the large-scale printing. Rheological properties are designed based on previous practical printing tests. The static and dynamic yield stress are 3289 Pa and 314.7 Pa, respectively. The plasticity viscosity is 32.5 Pa·s. The initial setting time is 59.2 mins. The flexural strengths are 8.6 MPa, 7.7 MPa, 7.4 MPa, 3.5 MPa, 2.1 MPa at 25 ℃ (ambient temperature), 200 ℃, 400 ℃, 600 ℃ and 800 ℃ respectively. The compressive strength are 64.9 MPa, 48.5 MPa, 48.8 MPa, 50.9 MPa, 31.8 MPa at 25 ℃, 200 ℃, 400 ℃, 600 ℃ and 800 ℃ respectively. The Young's modulus is 27.6 GPa at 25 ℃.

In the future, intensive work should be conducted to investigate the printability and fire performance of 3D printable materials. i.e. methods to improve the printability quality and printing speed should be studied, and the influence of elevated temperatures and fiber proportions on Young's modulus should be explored, and various fire-related properties such as permeability should be investigated. Besides, the fire rating test of 3D printed structure should be paid more attention, as it is an essential parameter for engineering applications.

Disclosure statement

No potential conflict of interest was reported by the authors.

Funding

The authors would like to acknowledge National Research Foundation, Prime Minister's Office, Singapore under its Medium Sized Centre funding scheme, Singapore Centre for 3D Printing and Sembcorp Design & Construction Pte Ltd for their funding and support in this research project.

Notes on contributions

Mr. Yiwei Weng obtained his B.E. in Materials Science and Engineering from University of Science and Technology Beijing. He is currently pursuing his PhD in School of CEE, under the supervision of Assistant Professor Shunzhi Qian (CEE) and co-supervisor Associate Professor Ming Jen Tan (MAE). His current research interests in the area of rheology of cementitious materials, the development of 3D printable cementitious materials and process optimization of 3D printing.

Dr. Mingyang Li is currently working as a postdoctoral research fellow in Building and Construction program of Singapore Centre for 3D Printing. He received his B.E. from Tsinghua University, M.E. from Beijing Jiaotong University, and Ph.D. from Missouri University of Science and Technology. His research interests are in the areas of Additive Manufacturing (AM) with emphasis on extrusion-based AM processes, and modeling and numerical simulation of heat transfer and fluid dynamics.

Mr. Zhixin Liu obtained his B.Eng. from Yantai University, China and M.Eng. from Beihang University, China. He is currently pursuing his PhD degree in Singapore Centre for 3D Printing at Nanyang Technological University. His research interest is 3D cementitious material printing under the supervision of Associate Professor Teck Neng Wong.

Mr. Wenxin Lao obtained his bachelor's degree in mechanical engineering at the University of Michigan-Shanghai Jiao Tong University Joint Institute in Shanghai Jiao Tong University, China. He completed his his M.S. degree in mechanical engineering at the University Hong Kong. He is pursuing his Ph.D. under the supervision of Associate Professor Tegoeh

Tjahjowidodo in the Mechanical Engineering at Nanyang Technological University. His current research focus on the nozzle's influence on the formation of cementitious material extrudate in the cementitious material 3D printing.

Mr. Bing Lu received his bachelor's degree at Southeast University, China. He is currently a Ph.D. research student in Singapore Centre for 3D Printing at Nanyang Technological University, Singapore. His current research interest is development of spray-based 3D printable cementitious materials.

Mr. Dong Zhang received his bachelor's and master's degree in Fire Protection Engineering from Central South University. He is currently pursuing his Ph.D. at School of Civil and Environmental Engineering in Nanyang Technological University (NTU), Singapore. His current research works focus on the fire resistance of ultra-high performance concrete.

Dr. Ming Jen Tan attended Anglo-Chinese School and Anglo-Chinese Junior College, Singapore and received both his B.Sc (Eng.) and Ph.D. from The Royal School of Mines, Imperial College, London. He was Japan Society for the Promotion of Science (JSPS) Fellow at Kyoto University in 1991, Science & Technology Agency (STA) Fellow at the Mechanical Engineering Laboratory (A.I.S.T., M.I.T.I.), Tsukuba, Japan 1992–93, Visiting Scientist at Columbia University (2003) and Fulbright Scholar (2004) at both The Anderson School (UCLA) and Kellogg School of Management (Northwestern University) in the United States of America.

References

Arioz, O.. 2007. "Effects of Elevated Temperatures on Properties of Concrete." *Fire Safety*

Journal 42(8): 516–522.

Bos, Freek, Wolfs Rob, Ahmed Zeeshan, and Theo Salet. 2016. "Additive Manufacturing of Concrete in Construction: Potentials and Challenges of 3D Concrete Printing." *Virtual and Physical Prototyping* 2759(October): 1–17. http://www.tandfonline.com/doi/full/10.1080/17452759.2016.1209867.

Bos, F., et al. 2016. "Additive Manufacturing of Concrete in Construction: Potentials and Challenges of 3D Concrete Printing." *Virtual and Physical Prototyping* 11(3): 209–25. https://www.tandfonline.com/doi/full/10.1080/17452759.2016.1209867 (April 8, 2017).

Chhabra, R.P., and J.F. Richardson. 1959. Non-Newtonian Flow and Applied Rheology *Non-Newtonian Fluid Behaviour*. http://www.sciencedirect.com/science/article/pii/B9780750685320000020.

Chua, Chee Kai, Kah Fai Leong, and Chu Sing Lim. 2003. *Rapid Prototyping: Principles and Applications*. Singapore: World Scientific.

Davtalab, Omid, Ali Kazemian, and Behrokh Khoshnevis. 2018. "Perspectives on a BIM-Integrated Software Platform for Robotic Construction through Contour Crafting." *Automation in Construction* 89(January): 13–23.

Dong, Zhang, Tan Kang Hai, and Dasari Aravind. 2018. "Role of Polymer Fibres in Prevention of Explorive Spalling in Ultra-High Performance Concrete." In *SiF 2018– The 10th International Conference on Structures in Fire FireSERT, Ulster University, Belfast, UK, June 6-8, 2018*, , 85–91.

Hambach, Manuel, and Dirk Volkmer. 2017. "Properties of 3D-Printed Fiber-Reinforced Portland Cement Paste." *Cement and Concrete Composites* 79: 62–70. http://www.sciencedirect.com/science/article/pii/S0958946516301093.

Jiang, Jingchao, Jonathan Stringer, Xun Xu, and Ray Y Zhong. 2018. "Investigation of Printable Threshold Overhang Angle in Extrusion-Based Additive Manufacturing for

377 Reducing Support Waste." *International Journal of Computer Integrated Manufacturing*:
378 1–9.
379 Khoury, G A. 1992. "Compressive Strength of Concrete at High Temperatures: A
380 Reassessment." *Magazine of concrete Research* 44(161): 291–309.
381 Le, Thanh T. et al. 2012. "Mix Design and Fresh Properties for High-Performance Printing
382 Concrete." *Materials and Structures* 45: 1221–32.
383 http://www.springerlink.com/index/10.1617/s11527-012-9828-z.
384 Li, Mingyang et al. 2016. "Modeling and Analysis of Paste Freezing in Freeze-Form Extrusion
385 Fabrication of Thin-Wall Parts via a Lumped Method." *Journal of Materials Processing*
386 *Technology* 237: 163–80.
387 Li, Mingyang, Lie Tang, Robert G Landers, and Ming C Leu. 2013. "Extrusion Process
388 Modeling for Aqueous-Based Ceramic Pastes—Part 2: Experimental Verification."
389 *Journal of Manufacturing Science and Engineering* 135(5): 51009.
390 Lim, Jian Hui, Biranchi Panda, and Quang-cuong Pham. 2018. "Improving Flexural
391 Characteristics of 3D Printed Geopolymer Composite with In-Process Steel Cable
392 Reinforcement Improving Flexural Characteristics of 3D Printed Geopolymer Composites
393 with in-Process Steel Cable Reinforcement." *Construction and Building Materials* 178:
394 32–41. https://doi.org/10.1016/j.conbuildmat.2018.05.010.
395 Lim, Jian Hui, Yiwei Weng, and Mingyang Li. 2018. "Effect of Fiber Reinforced Polymer on
396 Mechanical Performance of 3D Printed Cementitious Material." In *Proceedings of the 3nd*
397 *International Conference on Progress in Additive Manufacturing (Pro-AM 2018), ,* 44–
398 49.
399 Lim, S. et al. 2012. "Developments in Construction-Scale Additive Manufacturing Processes."
400 *Automation in Construction* 21(1): 262–68.
401 Liu, Jin-Cheng, and Kang Hai Tan. 2018. "Fire Resistance of Ultra-High Performance Strain

Hardening Cementitious Composite: Residual Mechanical Properties and Spalling Resistance." *Cement and Concrete Composites* 89: 62–75. http://linkinghub.elsevier.com/retrieve/pii/S095894651730985X.

Lowke, Dirk. 2018. "Thixotropy of SCC—A Model Describing the Effect of Particle Packing and Superplasticizer Adsorption on Thixotropic Structural Build-up of the Mortar Phase Based on Interparticle Interactions." *Cement and Concrete Research* 104(November 2017): 94–104.

Lu, Bing et al. 2018. "Effect of Spray-based Printing Parameters on Cementitious Material Distribution" In *Proceedings of the 29th Annual International Solid Freeform Fabrication Symposium – An Additive Manufacturing Conference, Accepted,* , 1989–2002.

Panda, Biranchi, and Ming Jen Tan. 2018. "Experimental Study on Mix Proportion and Fresh Properties of Fly Ash Based Geopolymer for 3D Concrete Printing." *Ceramics International* (February). http://linkinghub.elsevier.com/retrieve/pii/S0272884218305819.

Perrot, A., D. Rangeard, and A. Pierre. 2016. "Structural Built-up of Cement-Based Materials Used for 3D-Printing Extrusion Techniques." *Materials and Structures*: 1213–20. http://link.springer.com/10.1617/s11527-015-0571-0.

Roussel, N. 2006. "A Thixotropy Model for Fresh Fluid Concretes: Theory, Validation and Applications." *Cement and Concrete Research* 36: 1797–1806. http://www.sciencedirect.com/science/article/pii/S0008884606001657 (April 10, 2017).

Ruan, S, and C Unluer. 2017. "Influence of Supplementary Cementitious Materials on the Performance and Environmental Impacts of Reactive Magnesia Cement Concrete." *Journal of Cleaner Production* 159: 62–73. http://dx.doi.org/10.1016/j.jclepro.2017.05.044.

Ruan, S., Qiu J., Yang E., and Cise Unluer. 2018. "Fiber-Reinforced Reactive Magnesia-Based

Tensile Strain-Hardening Composites." *Cement and Concrete Composites* 89: 52–61.

Salet, Theo A M, Zeeshan Y Ahmed, Freek P Bos, and Hans L M Laagland. 2018. "Design of a 3D Printed Concrete Bridge by Testing Design of a 3D Printed Concrete Bridge by Testing." *Virtual and Physical Prototyping* 2759(May): 1–15. http://www.tandfonline.com/action/journalInformation?journalCode=nvpp20%0Ahttps://doi.org/10.1080/17452759.2018.1476064.

Soltan, Daniel G., and Victor C. Li. 2018. "A Self-Reinforced Cementitious Composite for Building-Scale 3D Printing." *Cement and Concrete Composites* 90(July 2018): 1–13.

T.Pham, Long, and Nocholas J.Carino. 2012. "Fire Performance of High Strength Concrete: Research Needs." *Advanced Technology in Structural Engineering*.

Tang, S., Yan Yao, Carmen Andrade, and Z J Li. 2015. "Recent Durability Studies on Concrete Structure." *Cement and Concrete Research* 78: 143–54.

Tay Y. et al. 2017 a. "3D Printing Trends in Building and Construction Industry: A Review." *Virtual and Physical Prototyping* 12(3): 261–76.

Tay Y. et al. 2018. "Time Gap Effect on Bond Strength of 3D-Printed Concrete." *Virtual and Physical Prototyping* 0(0): 1–10. https://doi.org/10.1080/17452759.2018.1500420.

Wang Q. et al.. 2018. "A Solid Oxide Fuel Cell (SOFC)-Based Biogas-from-Waste Generation System for Residential Buildings in China: A Feasibility Study." *Sustainability* 10(7): 2395.

Weng, Yiwei et al. 2016. "Rheology and Printability of Enginggered Cementitious Composites- a Literature Review." In *Proceedings of the 2nd International Conference on Progress in Additive Manufacturing (Pro-AM 2016), ,* 427–32.

Weng, Y. et al. 2018 a. "Empirical Models to Predict Rheological Properties of Fiber Reinforced Cementitious Composites for 3D Printing." *Construction and Building Materials* 189: 676–685. https://doi.org/10.1016/j.conbuildmat.2018.09.039.

Weng, Y. et al. 2018 b. “Design 3D Printing Cementitious Materials via Fuller Thompson Theory and Marson-Percy Model.” *Construction and Building Materials* 163: 600–610. http://doi.org/ 10.1080/17452759.2018.1476064

Weng, Y. et al. 2018. “3D Printable High Performance Fiber Reinforced Cementitious Composites for Large-Scale Printing.” *Proceedings of the 3nd International Conference on Progress in Additive Manufacturing (Pro-AM 2018)* (May): 19–24.

Wolfs, R J M, F P Bos, and T A M Salet. 2018. “Early Age Mechanical Behaviour of 3D Printed Concrete : Numerical Modelling and Experimental Testing.” *Cement and Concrete Research* 106(May 2017): 103–16.

Xia, Ming, and Jay Sanjayan. 2016. “Method of Formulating Geopolymer for 3D Printing for Construction Applications.” *Materials and Design* 110: 382–90.

Xia, Ming, and Jay G Sanjayan. 2018. “Methods of Enhancing Strength of Geopolymer Produced from Powder- Based 3D Printing Process.” *Materials Letters* 227: 281–83. https://doi.org/10.1016/j.matlet.2018.05.100.

Yang, E., M Sahmaran, Yang Y., and VC Li. 2009. “Rheological Control in Production of Engineered Cementitious Composites.” *ACI Materials Journal* 106(4): 357–66.

Zhang, Dong, Aravind Dasari, and Kang Hai Tan. 2018. “On the Mechanism of Prevention of Explosive Spalling in Ultra-High Performance Concrete with Polymer Fibers.” *Cement and Concrete Research*.

Zhang, Xu et al. 2018. “Large-Scale 3D Printing by a Team of Mobile Robots.” *Automation in Construction* 95: 98–106.

Zheng, W. et al.. 2014. “Microstructure and Mechanical Properties of RPC Containing PP Fibres at Elevated Temperatures.” *Magazine of Concrete Research* 66(8): 397–408. http://www.icevirtuallibrary.com/doi/10.1680/macr.13.00232.